

Effects of water vapor addition on the laminar burning velocity of methane oxygen-enhanced flames at atmospheric pressure

A. Mazas^{*1,2}, D. Lacoste¹, B. Fiorina¹ and T. Schuller¹

¹ Laboratoire EM2C, CNRS and Ecole Centrale Paris, Grande Voie des Vignes, F-92295 Châtenay-Malabry, France.

² Air Liquide, Centre de Recherche Claude-Delorme, Les Loges-en-Josas, BP 126, F-78350 Jouy-en-Josas, France.

Abstract

Effects of water vapor addition on premixed methane oxygen-enhanced combustion are investigated through experiments and numerical simulations on laminar burning velocities of $\text{CH}_4/\text{O}_2/\text{N}_2/\text{H}_2\text{O}_{(v)}$ mixtures, carried out at atmospheric pressure and for a fixed inlet temperature $T_u = 373$ K. The mixture equivalence ratio is varied from 0.6 to 1.5, the molar oxygen-enrichment ratio of the oxidizer $\text{O}_2/(\text{O}_2+\text{N}_2)$ from 0.21 (air) to 0.50 and the water vapor molar fraction from 0 to 0.45. Experimental data yield a linear decrease of the laminar burning velocity when the water vapor molar fraction is increased. This linear decrease is well predicted by the computation. For an oxygen-enrichment ratio in the oxidizer $\text{O}_2/(\text{O}_2+\text{N}_2)$ (mol.) equal to 0.5, this decrease is found to be independent of the equivalence ratio and a correlation is proposed to describe the effects of water vapor on the laminar burning velocity.

Introduction

In the last decade, oxy-combustion has received particular attention. Technologies in which the fuel is burned with pure oxygen or oxygen-enriched air have been identified as a promising approach to reducing greenhouse gas emissions. Using oxygen as an oxidant instead of air enables to substantially increase CO_2 concentration in the burned gases, facilitating its capture and then its storage [1]. In most cases, oxygen has to be diluted with recycled flue gases to maintain exhaust temperatures compatible with the materials thermal resistance.

At the same time, oxy-combustion has been increasingly used to improve processes energy efficiency, enabling a significant reduction of fuel consumption. Moreover, highly-diluted oxy-combustion regimes have been identified as a successful way of limiting NO_x emissions [2]. As water vapor is a key component of combustion products, it is thus valuable to analyze the influence of water steam in oxy-combustion or oxygen-enhanced combustion processes.

A few prior studies have examined effects of water steam addition on premixed and non-premixed flames properties. Water vapor dilution has first been identified as a successful way to lower pollutant emissions in gas turbines operating both in premixed and non-premixed modes [3]. It was shown that water steam addition in various combustible mixtures (natural gas, *n*-heptane, *iso*-octane) led to substantial reductions of NO_x emissions [4, 5]. Operating at constant adiabatic flame temperature, dilution with water vapor was found to reduce NO_x levels by more than a factor of two compared to nitrogen dilution [6]. Impact of water steam dilution on CO emissions was also examined and discussed [4, 5].

The influence of water steam as a fire inhibitor in premixed methane-air flames has also been investigated. Regarding the thermal suppression effect, water vapor was found to be more effective than other gaseous thermal agents (N_2 and CF_4) or some chemical agents (CF_3Br) but less effective than the same mass of water mist [7]. These studies are however mainly based on numerical simulations; corresponding experiments were limited yet to small quantities of added water vapor [7, 8]. Studies on inhibition of premixed flames by the means of various types of diluents can be closely linked to the present study since the reduction in laminar burning velocity can be used as a relevant indicator of the effectiveness of an inhibiting agent [9].

The effects of water vapor addition on flame extinction and ignition have also been examined recently. Critical conditions of ignition and extinction for hydrogen and methane flames were measured and calculated as a function of the water mass fraction in the oxidizer [10]. It was observed that steam addition favors extinction and narrows regimes of ignition for premixed and non-premixed flames. Moreover, it is worth noting that the elementary reactions examined in the pre-cited work showed a weak sensitivity to water addition. This was for example investigated in Ref. [11]. Thanks to auto-ignition delays and species concentrations measurements, chemical kinetic modeling was improved to include the reactions that play a significant role in the kinetic of oxidation of fuels in presence of water vapor.

Laminar burning velocities of methane-air flames diluted with water steam were measured with spherically expanding flames in a constant volume vessel for $\text{CH}_4/\text{air}/\text{H}_2\text{O}_{(v)}$ mixtures [12]. Measurements were carried out for stoichiometric mixtures over a wide range of initial pressures and for a constant unburned gas temperature T_u of 473 K, with a water vapor molar fraction varying from 0 to 0.2. Burning velocities were deduced from direct photographs of the early stage of the flame propagation. Results at atmospheric pressure show a linear decrease of the burning velocity when the water vapor molar fraction is increased, but data were not reported yet for non-stoichiometric or oxygen-enriched mixtures.

Specific objectives

Detailed understanding of water steam addition in oxy-combustion technologies is required to improve these processes. Experiments and simulations are conducted in this work to examine the effects of water vapor addition on the laminar burning velocity of oxygen-enhanced methane flames at atmospheric pressure for water vapor concentrations covering the range of operating conditions in practical applications.

Experimental setup

Experiments were conducted on an oxycombustion-dedicated set-up represented in Fig. 1. This set-up comprises gas feeding lines, a humidifier used to produce water vapor and an axisymmetric burner on which steady conical laminar premixed $\text{CH}_4/\text{O}_2/\text{N}_2/\text{H}_2\text{O}_{(v)}$ flames are stabilized.

Methane (CH_4), oxygen (O_2), and nitrogen (N_2) gases (purity > 99.99 %) are supplied from an external network of tanks. Flow rates of CH_4 , O_2 , N_2 are regulated with calibrated mass flow controllers (Bronkhorst F-Series). The water va-

^{*}Corresponding author: antoine.mazas@airliquide.com
Proceedings of the European Combustion Meeting 2009

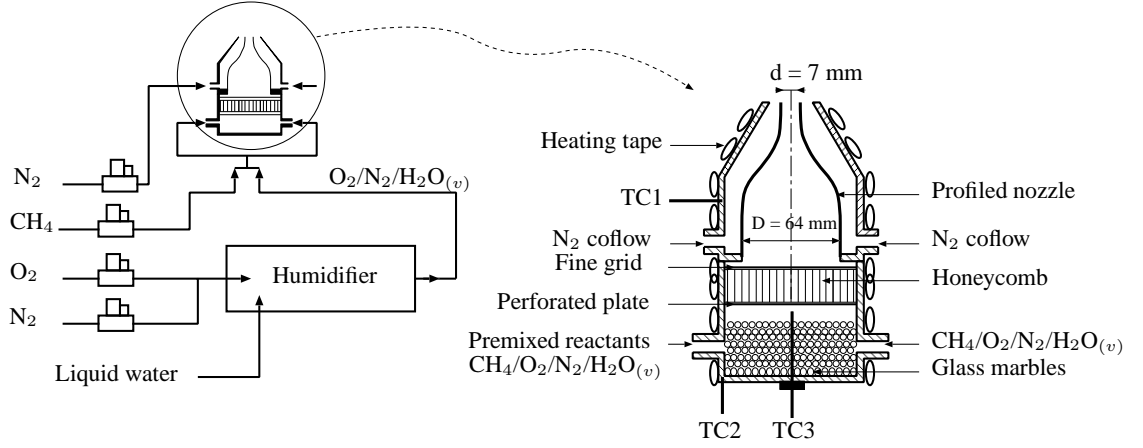


Figure 1: Schematic of the experimental facility dedicated to premixed oxy-combustion. Left: overview of the global set-up. Right: detailed view of the burner.

por is produced with a custom-built humidifier, derived from a Cellkraft P-50 humidifier. Steam production is based on the humidification of a carrier gas by transfer of water vapor through a specific membrane. The carrier gas is composed of O_2 and N_2 , which are beforehand premixed according to the chosen composition of the oxidizer. This carrier gas flows in membrane tubes, which are immersed in demineralized liquid water heated with electrical resistances. The carrier gas flows out saturated with water vapor, the humidity of the obtained $O_2/N_2/H_2O(v)$ mixture depending on the temperature of the liquid water surrounding the membrane tubes. The dew point temperature T_{dew} of the humidified gas is then measured with a humidity sensor (Vaisala). A closed loop control of humidity based on the measured dew point temperature is used to regulate the temperature of liquid water. This allows to reach the desired humidity of the $O_2/N_2/H_2O(v)$ mixture. The humidified mixture is finally heated to the unburned gases desired temperature T_u set to 373 K in these experiments. The molar fraction of water vapor X_{H_2O} in this mixture is directly inferred from the saturation vapor pressure $p_{sat}(T_{dew})$ and from the humidifier inner pressure p_h , which is measured with a high temperature pressure transducer placed at the humidifier exit:

$$X_{H_2O} = \frac{p_{H_2O}}{p_h} = \frac{p_{sat}(T_{dew})}{p_h} \quad (1)$$

Figure 2 shows the mass of evaporated water as a function of time for two dew point temperatures $T_{dew} = 320$ K and 345 K, and for two carrier gas mass flow rates $\dot{m}_{cg} = 10$ nL/min and 30 nL/min. Measurements are compared with theoretical evaporated water masses calculated with Eq. 1. Results show that the evaporated water mass is in excellent agreement with the theoretical predictions within 1% accuracy. It can be concluded from the humidifier linear operation and from the excellent repeatability of these tests that the water steam concentration is remarkably stable and accurately controlled.

The temperature of all the components downstream the humidifier is regulated at $T_u = 373$ K to prevent water condensation. The $O_2/N_2/H_2O(v)$ mixture and methane CH_4 flow are then premixed before being injected in the axisymmetric burner. Gases are injected in the lower part of the burner, which is filled with glass marbles (1 to 3 mm diameter) to further reduce possible mixture non-homogeneities. The reactive mixture then flows successively through a perforated plate, a honeycomb structure and a refined metallic grid to obtain a

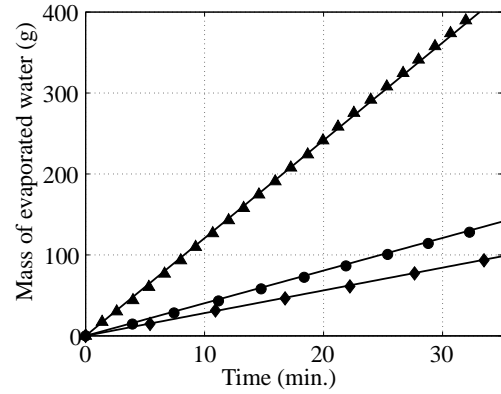


Figure 2: Experimental (symbols) and theoretical (lines) mass of evaporated water as a function of time for different dew point temperatures T_{dew} and carrier gas mass flow rates \dot{m}_{cg} . (◆) $T_{dew} = 320$ K and $\dot{m}_{cg} = 30$ nL/min. ; (●) $T_{dew} = 345$ K and $\dot{m}_{cg} = 10$ nL/min. ; (▲) $T_{dew} = 345$ K and $\dot{m}_{cg} = 30$ nL/min.

laminar flow entering the inlet of the profiled converging nozzle, of contraction ratio $\sigma = (D/d)^2 = 86$. This converging nozzle is used to reduce the boundary layer thickness by accelerating the flow and obtain a top hat velocity profile at the burner outlet of diameter $d = 7$ mm. Finally, a small co-flow of nitrogen surrounding the inner main nozzle is used to prevent potential outer perturbations. The velocity profile at the burner outlet was characterized using a hot wire anemometry system (Dantec). It was checked that the velocity profile remains flat over 5 mm and the RMS fluctuations were found to be less than 1.0 % of the mean velocity. This nearly uniform velocity profile is decisive for laminar burning velocity measurements, as it is discussed below.

The burner temperature is regulated with electrical heating tapes and the temperature field homogeneity is simultaneously controlled with a J-type thermocouple TC1 inserted in the burner body close to the top and with a K-type thermocouple TC2 inserted in the bottom plate of the burner. A K-type thermocouple TC3 located immediately upstream the perforated plate is used to measure the mixture temperature T_u .

Laminar burning velocity measurements and calculations

The laminar burning velocity s_u^o is defined as the velocity at which a laminar, stationary, plane, unstretched, adiabatic flame moves relative to the unburned premixed gas in a direction normal to the flame surface. However, a flame fulfilling the pre-cited requirements cannot be easily obtained experimentally. Significant efforts have been made to develop experimental techniques leading to accurate measures of laminar burning velocities [13]. Among those techniques are the conical flame method, the flat and one-dimensional flame method, the outwardly propagating spherical flame method and the stagnation flame method with a counterflow twin-flame configuration. For a given reactive mixture, the suitable method depends on the range of burning velocities to be explored. It is known that increasing the oxygen molar fraction in the oxidizer substantially raises the burning velocity [14]. Due to those expected high values, it was chosen to work with steady conical $\text{CH}_4/\text{O}_2/\text{N}_2/\text{H}_2\text{O}_{(v)}$ flames stabilized over the burner outlet. Despite a few disadvantages discussed below, the conical flame method is easy to implement and provides reliable results. Assuming the whole reactive mixture is burnt, one can define an average laminar flame speed \bar{s}_u that can be calculated from the mass conservation equation:

$$\dot{m} = \rho_u \bar{s}_u \mathcal{A}_f \quad (2)$$

where \dot{m} is the reactants mass flow rate, ρ_u is the unburned gas density and \mathcal{A}_f is the flame surface area. The choice of the flame surface area \mathcal{A}_f is of particular importance for the determination of the burning velocity [15]. Since the laminar burning velocity s_u^o is defined relative to the unburned gases, the most appropriated area is the upstream boundary of the preheat zone that can be determined with a Schlieren technique. When using a Schlieren imaging set-up, the light deflection due to optical index gradients is in first approximation proportional to $|\nabla T|/T^2$, where T is the gas temperature [16]. As the maximum of light deflection occurs close to the upstream boundary of the preheat zone, the Schlieren technique is an efficient diagnostic to measure laminar burning velocities [17, 18].

The quality of burning velocity measurements is very sensitive to the velocity profile at the burner exit. Indeed, a uniform velocity profile ensures that the local flame speed s_u is constant over most of the flame cone [14]. Flames obtained in this work - as well as their Schlieren boundary - are nearly straight-sided cones as shown in Fig. 3. Schlieren images are obtained using a classical Z-arrangement with long focal lengths mirrors and vertical knives to measure horizontal gradients. These images are then post-processed using an edge detection algorithm based on Sobel operator to determine the upstream boundary of the preheat zone. The average laminar flame speed \bar{s}_u can finally be deduced from the measure of the half cone angle α (as defined in Fig. 3) and from the unburned gas mean velocity \bar{v} using the relation:

$$\bar{s}_u = \bar{v} \sin(\alpha) \quad (3)$$

However, this quantity measured with the methodology described above does not exactly match with the laminar burning velocity s_u^o , mainly due to stretch effects [19, 20]. Stretch effects due to hydrodynamic strain along the flame front are not compensated in this study and will be the subject of further investigations. However, these effects are limited since velocity gradients along the flame are small for conical flames stabilized in uniform flows. Stretch effects due to curvature

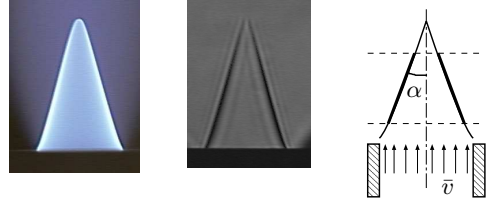


Figure 3: Left: direct photograph of $\text{CH}_4/\text{O}_2/\text{N}_2$ flame, with $\text{O}_2/(\text{O}_2+\text{N}_2)$ (mol.) = 0.50 and $\phi = 1.50$, at $T_u = 373$ K and atmospheric pressure. Center: corresponding Schlieren image. Right: schematic representation of the method used to measure the half cone angle.

are predominant in these experiments because the flames are small. In order to maintain the same field of curvature in all experiments, the ratio of the flame height over the burner diameter H/d was kept unchanged (within $\sim 5\%$). In what follows, we use "laminar flame speed" to designate the measured average burning velocity \bar{s}_u introduced previously.

These experiments were completed by simulations of one-dimensional, freely propagating, unstretched, adiabatic, laminar, premixed flames using the PREMIX code of the CHEMKIN package [21]. This complex chemistry one-dimensional flame solver, based on a second order numerical scheme and Newton iteration, was employed with the detailed kinetic mechanism GRI mech. 3.0 [22]. This mechanism includes 325 elementary chemical reactions, involving 53 species with their thermodynamic and transport properties. Calculations were performed considering also differential diffusion effects.

Results

Laminar flame speeds of $\text{CH}_4/\text{O}_2/\text{N}_2/\text{H}_2\text{O}_{(v)}$ mixtures are measured over a wide range of operating conditions, for a constant unburned gas temperature $T_u = 373 \text{ K} \pm 1 \text{ K}$. The parameters examined in this work are the oxygen-enrichment ratio in the oxidizer $\Omega = \text{O}_2/(\text{O}_2+\text{N}_2)$ (mol.), the water vapor molar fraction $X_{\text{H}_2\text{O}}$ and the mixture equivalence ratio ϕ , defined as:

$$\phi = \left(\frac{\dot{m}_{\text{CH}_4}}{\dot{m}_{\text{O}_2}} \right) / \left(\frac{\dot{m}_{\text{CH}_4}}{\dot{m}_{\text{O}_2}} \right)_s \quad (4)$$

where $(\dot{m}_{\text{CH}_4}/\dot{m}_{\text{O}_2})_s$ is the ratio of fuel to oxygen at stoichiometry.

The methodology developed is first validated with well documented methane-air flames at $T_u = 298 \text{ K}$ and at atmospheric pressure. Laminar flame speeds are measured for mixture equivalence ratios varying from 0.9 to 1.4, as shown in Fig. 4. Leaner CH_4 /air regimes cannot be obtained using this set-up dedicated to oxy-combustion. Results are compared with numerical simulations and with reference measurements obtained using Laser Doppler Velocimetry and Particle Image Velocimetry [23, 24]. A good agreement is found between the different experimental results, as well as with the computed burning velocities.

The influence of water vapor on the laminar burning velocity of methane flames is now examined. Because of the difficulty to stabilize conical methane-air flames with high water vapor concentrations, the oxidizer is first slightly enriched with oxygen. Figure 5 shows the evolution of the laminar flame speed when the water vapor molar fraction is increased from 0 to about 0.2, for a stoichiometric mixture $\phi = 1.0$ and for an oxygen-enrichment ratio of the oxidizer $\Omega = 0.30$. The

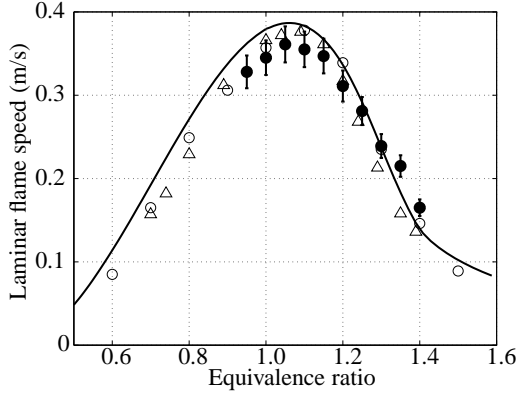


Figure 4: Experimental (symbols) and computed (lines) laminar flame speeds of CH_4/air mixtures, for $\text{O}_2/(\text{O}_2+\text{N}_2)$ (mol.) = 0.21, at $T_u = 298$ K and atmospheric pressure. (●) present work; (○) Vagelopoulos et al. (1998); (△) Dong et al. (2003).

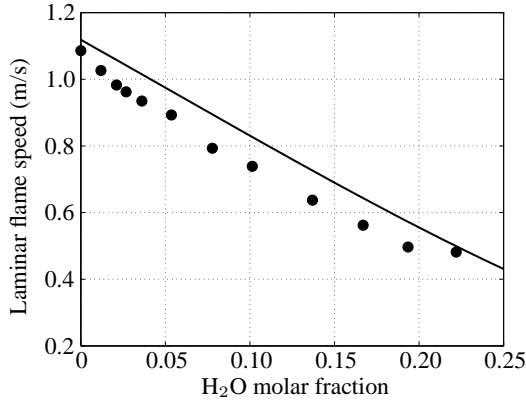


Figure 5: Experimental (symbols) and computed (lines) laminar flame speeds of $\text{CH}_4/\text{O}_2/\text{N}_2/\text{H}_2\text{O}_{(v)}$ mixtures, for $\phi = 1.0$ and $\text{O}_2/(\text{O}_2+\text{N}_2)$ (mol.) = 0.30, at $T_u = 373$ K and atmospheric pressure.

laminar flame speed decreases linearly when the water steam molar fraction is increased. The agreement between experimental results and GRI mech. 3.0 predictions is within 7%. Although the laminar burning velocity of the dry $\text{CH}_4/\text{O}_2/\text{N}_2$ mixture is overestimated by numerical calculations, the slope of the straight line defined by the experimental data is correctly predicted by the GRI mech. 3.0 kinetic mechanism.

Effects of water steam dilution are now examined for a higher oxygen-enrichment ratio Ω in the oxidizer. Figure 6 shows the results obtained when the oxygen molar fraction in the oxidizer is increased to $\Omega = 0.50$, and for three different equivalence ratios $\phi = 0.60$, 1.0 and 1.50 respectively. As observed previously, the laminar flame speed evolves linearly when the water vapor molar fraction is increased from 0 to 0.45. Solid lines in Fig. 6 indicate the computed burning velocities, that show a similar linear dependence with water vapor addition. For a stoichiometric mixture $\phi = 1.0$, numerical simulations match very well with experimental results. For lean mixtures ($\phi = 0.60$), the laminar burning velocity also linearly decreases when increasing the water vapor molar fraction from 0 to 0.28. It is observed in this case that the GRI mech. 3.0 overpredicts the measured laminar flame speeds by $\sim 11\%$, but slopes of measured and computed burning veloci-

ties are identical. Consequently, it seems that, despite an over prediction of the burning velocity without water vapor, effects of water steam addition are correctly taken into account by the GRI mech. 3.0. The laminar burning velocity is finally measured and computed for rich mixtures. As shown in Fig. 6, the same linear trend is observed when the water molar fraction is varied from 0 to 0.3, for a rich mixture where $\phi = 1.50$. In this configuration, it is observed that the GRI mech. 3.0 underpredicts the measured flame speeds by $\sim 20\%$. However, as for lean mixtures, slopes of measured and computed burning velocities are found to be equal.

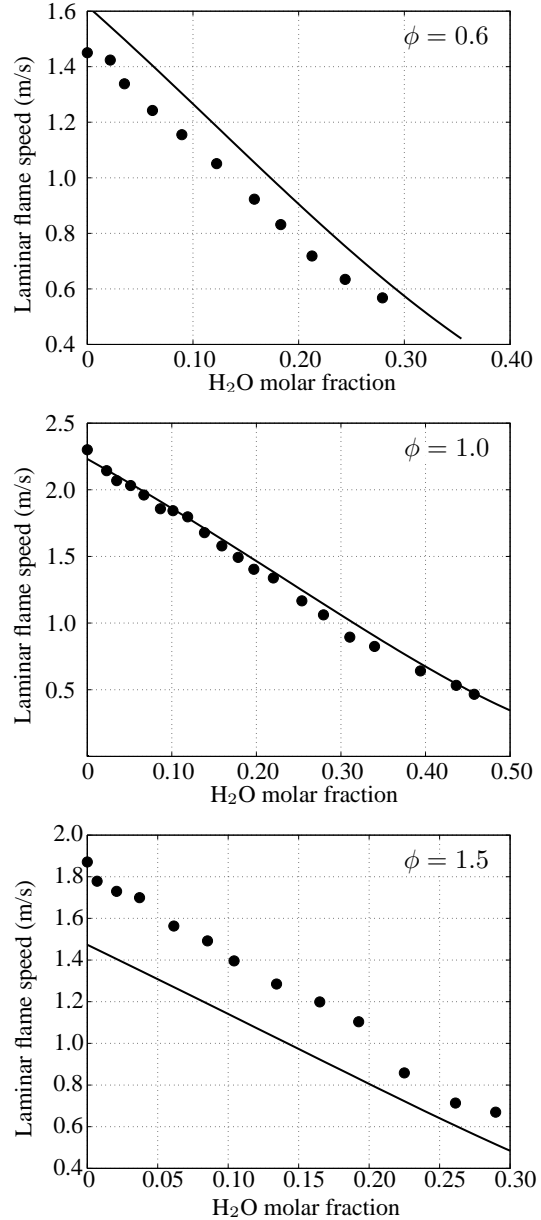


Figure 6: Experimental (symbols) and computed (lines) laminar flame speeds of $\text{CH}_4/\text{O}_2/\text{N}_2/\text{H}_2\text{O}_{(v)}$ mixtures, for $\text{O}_2/(\text{O}_2+\text{N}_2)$ (mol.) = 0.50, at $T_u = 373$ K and atmospheric pressure. From top to bottom: $\phi = 0.60$, $\phi = 1.0$ and $\phi = 1.50$.

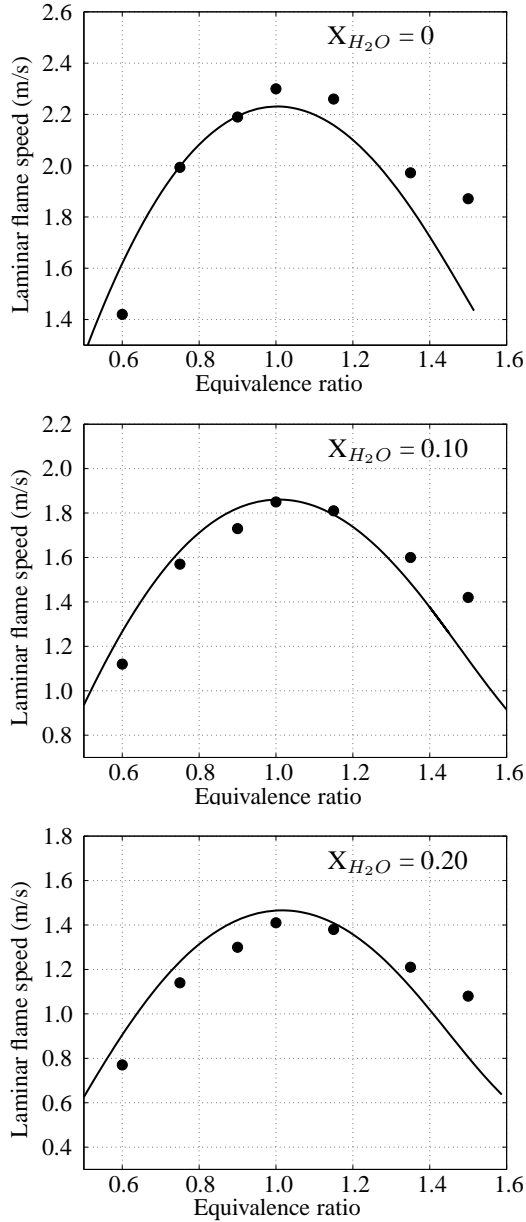


Figure 7: Experimental (symbols) and computed (lines) laminar flame speeds of $\text{CH}_4/\text{O}_2/\text{N}_2/\text{H}_2\text{O}_{(v)}$ mixtures, for $\text{O}_2/(\text{O}_2+\text{N}_2)$ (mol.) = 0.50, at $T_u = 373$ K and atmospheric pressure. From top to bottom: $X_{\text{H}_2\text{O}} = 0$, $X_{\text{H}_2\text{O}} = 0.10$ and $X_{\text{H}_2\text{O}} = 0.20$.

Flame speeds are plotted in Fig. 7 as a function of the equivalence ratio ϕ , for an oxygen-enrichment ratio in the oxidizer $\Omega = 0.50$ and for three different molar fractions of water vapor: $X_{\text{H}_2\text{O}} = 0$, $X_{\text{H}_2\text{O}} = 0.10$ and $X_{\text{H}_2\text{O}} = 0.20$. Experimental data obtained for a fixed equivalence ratio with an increasing water vapor molar fraction were interpolated to obtain the symbols presented in Fig. 7. It is observed that experimental and numerical results are in excellent agreement near stoichiometry, independently of the water vapor concentration in the initial mixture. As exposed previously, the GRI mech. 3.0 predictions are found to be slightly higher than the measured laminar flame speeds for very lean mixtures while the mechanism underestimates rich mixtures burning velocities.

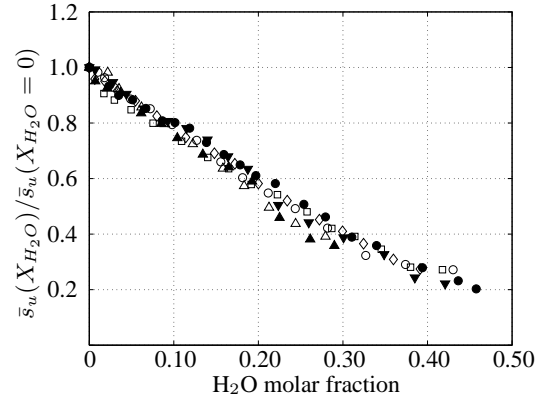


Figure 8: Normalized flame speeds for $\text{O}_2/(\text{O}_2+\text{N}_2)$ (mol.) = 0.50 and for different equivalence ratios. (\triangle) $\phi = 0.60$, (\circ) $\phi = 0.75$, (\diamond) $\phi = 0.90$, (\bullet) $\phi = 1.0$, (\square) $\phi = 1.15$, (\blacktriangledown) $\phi = 1.35$, (\blacktriangle) $\phi = 1.50$.

Discussion

Adding a diluent in a reactive mixture modifies the combustion properties. Depending on the diluent physical and chemical characteristics, a dilution process lead to changes in mixture heat capacity, in exothermicity, and in heat and mass diffusion phenomena. In addition to modifications of the thermophysical properties, dilution may also affect significantly the elementary chemical reactions taking place in the reaction zone. One of the major issues of studying the impact of a diluent on the flame properties is to determine whether the considered dilution has mainly a thermodynamical effect or if it also modifies the chemical kinetics. Since the H_2O molecule is likely to produce highly reactive elementary radicals like H, O or OH, it is interesting to discuss the impact of water vapor addition on methane oxygen-enhanced premixed flames. To that purpose, Fig. 8 plots the normalized value of laminar flame speeds as a function of the water vapor molar fraction, for a given oxygen-enrichment ratio $\Omega = 0.50$ and different equivalence ratios. It is observed that the experimental data collapse on a single curve. A correlation can then be proposed for $\text{CH}_4/\text{O}_2/\text{N}_2/\text{H}_2\text{O}_{(v)}$ mixtures:

$$\frac{\bar{s}_u(X_{\text{H}_2\text{O}})}{\bar{s}_u(X_{\text{H}_2\text{O}} = 0)} = 1 - C X_{\text{H}_2\text{O}} \quad (5)$$

where the coefficient C was found to be equal to $C = 1.86$ in these experiments. This correlation is valid for an oxygen-enrichment ratio $\Omega = 0.50$, equivalence ratios comprised between $0.6 < \phi < 1.5$ and for water vapor molar fractions in the range $0 < X_{\text{H}_2\text{O}} < 0.4$. For these conditions, dilution of $\text{CH}_4/\text{O}_2/\text{N}_2$ flames by water vapor is found to be independent of the equivalence ratio. It can be inferred from this result that the chemical impact of water vapor dilution on $\text{CH}_4/\text{O}_2/\text{N}_2$ flames relative to laminar burning velocities is limited even for high water vapor concentrations.

Conclusions

Effects of water vapor on the laminar burning velocity of $\text{CH}_4/\text{O}_2/\text{N}_2/\text{H}_2\text{O}_{(v)}$ mixtures were investigated over a wide range of operating conditions, for an unburned reactants temperature of 373 K and at atmospheric pressure. Laminar flame speeds were measured with the conical flame method thanks to a Schlieren apparatus, with a constant flame height to burner diameter ratio H/d to keep a constant curvature. Experimental results are compared to computed laminar burning velocities using the detailed kinetic mechanism GRI mech. 3.0. For all conditions explored, it is found that the burning velocity decreases linearly when the water vapor fraction is increased. The slope of the line defined by the experimental results is accurately predicted by the GRI mech. 3.0. A good agreement between measurements and calculations is found for stoichiometric mixtures. For an oxygen enrichment-ratio in the oxidizer $\text{O}_2/(\text{O}_2+\text{N}_2)$ (mol.) = 0.50, the laminar burning velocity is over predicted for lean mixtures while it is underestimated for rich mixtures. Furthermore, the decrease of the burning velocity for an increasing vapor molar fraction is found to be independent of the equivalence ratio, for a given oxidizer composition.

This highlights that the effect of water steam addition on the laminar burning velocity of $\text{CH}_4/\text{O}_2/\text{N}_2$ mixtures is mainly thermodynamical while flame chemicals is weakly affected. This dilution phenomenon has now to be confirmed for higher oxygen concentrations in the oxidizer, including the case of full-oxycombustion.

Acknowledgments

This work was supported by Air Liquide, under the technical monitoring of Dr. B. Labégorre, and by Agence Nationale pour la Recherche et la Technologie (ANRT).

References

- [1] J. D. Figueroa, T. Fout, S. Plasynski, H. McIlvried, and R. D. Srivastava. *Int. J. Green. Gas Cont.* 2 (2008) 9–20.
- [2] A. Cavaliere and M. de Joannon. *Prog. Energy Combust. Sci.* 30 (2004) 329–366.
- [3] S. M. Correa. In *Twenty-Seventh Symposium (International) on Combustion*, The Combustion Institute (1998) pp. 1793–1813.
- [4] A. Bhargava, M. Colket, W. Sowa, K. Casleton, and D. Maloney. *J. Eng. Gas Turb. Power - Trans. ASME* 122 (2000) 405–411.
- [5] B. de Jager, J. B. W. Kok, and G. Skevis. *Proc. Combust. Inst.* 31 (2007) 3123–3130.
- [6] M. J. Landman, M. A. F. Derksen, and J. B. W. Kok. *Combust. Sci. Technol.* 178 (2006) 623–634.
- [7] S. P. Fuss, E. F. Chen, W. H. Yang, R. J. Kee, B. A. Williams, and J. W. Fleming. *Proc. Combust. Inst.* 29 (2002) 361–368.
- [8] G. O. Thomas. *Combust. Flame* 130 (2002) 147–160.
- [9] G. T. Linteris and L. Truett. *Combust. Flame* 105 (1996) 15 – 27.
- [10] R. Seiser and K. Seshadri. *Proc. Combust. Inst.* 30 (2005) 407–414.
- [11] T. Le Cong and P. Dagaut. *ASME paper #GT2008-50272* (2008) .
- [12] V. S. Babkin and A. V. V'yun. *Fizika Goreniya i Vzryva* 7 (1971) 392–395.
- [13] C. J. Rallis and A. M. Garforth. *Prog. Energy Combust. Sci.* 6 (1980) 303–329.
- [14] B. Lewis and G. Von Elbe. *Combustion, Flames and Explosions of Gases* (1987) Academic Press, 3rd ed, New York.
- [15] A. G. Gaydon and H. G. Wolfhard. *Flames* (1970) Chapman and Hall, London.
- [16] G. S. Settles. *Schlieren and Shadowgraph Techniques* (2001) Springer-Verlag, Berlin.
- [17] D. Dunn-Rankin and F. Weinberg. *Combust. Flame* 113 (1998) 303–311.
- [18] D. Durox and S. Ducruix. *Combust. Flame* 120 (2000) 595–598.
- [19] G. H. Markstein. *Nonsteady Flame Propagation* (1964) Pergamon, New York.
- [20] C. K. Law. and C. J. Sung. *Prog. Energy Combust. Sci.* 26 (2000) 459-505.
- [21] J. Kee, K. Grcar, M.D. Smooke, and J.A. Miller. PRE-MIX: A Fortran program for modelling steady laminar one-dimensional premixed flames, Technical report, SANDIA National Laboratories (1985).
- [22] G. P. Smith, D. M. Golden, M. Frenklach, N. W. Morarty, B. Eiteneer, M. Goldenberg, C. T. Bowman, R. K. Hanson, S. Song, W. C. Gardiner, Jr., V. V. Lissianski, and Z. Qin. http://www.me.berkeley.edu/gri_mech/
- [23] C. M. Vagelopoulos and F. N. Egolfopoulos. *Proc. Combust. Inst.* 27 (1998) 513–519.
- [24] Y. F. Dong, C. M. Vagelopoulos, G. R. Spedding, and F. N. Egolfopoulos. *Proc. Combust. Inst.* 29 (2003) 1419–1426.